Regional variation in undulatory kinematics of two hammerhead species: the bonnethead (*Sphyrna tiburo*) and the scalloped hammerhead (*Sphyrna lewini*)

[1]Hoffmann, S.L., [2]Warren, S.M., [1]Porter, M.E.

[1]Florida Atlantic University, Department of Biological Sciences, 777 Glades Rd, Boca Raton, FL 33431
[2]Florida Atlantic University Department of Ocean and Mechanical Engineering, 777 Glades Rd, Boca Raton, FL 33431

Author for correspondence:
Sarah L. Hoffmann
Email: shoffmann2014@fau.edu

Keywords: frequency, amplitude, second moment of area, swimming velocity, cephalofoil

Summary statement:
During swimming, the scalloped hammerhead and bonnethead shark have similar kinematic outputs but different undulatory patterns. Flexion frequency and amplitude vary along the length of the body, whereas only amplitude varied between species.

Abstract

Hammerhead sharks (Sphyrnidae) are have a large amount of morpholigcal variation within the family, making them the focus of many studies. The size of the laterally expanded head, or cephalofoil, is inversely correlated with pectoral fin area. The inverse relation in cephalofoil and pectoral fin size in this family suggests that they might serve a complimentary role in lift generation. The cephalofoil is also hypothesized to increase olfaction, electroreception, and vision; however, little is known about how morphological variation impacts post-cranial swimming kinematics. Previous studies demonstrate that the bonnethead and scalloped hammerhead have significantly different yaw amplitude and we hypothesized that these species utilize varied frequency and amplitude of undulation along the body. We analyzed video of free swimming sharks to examine kinematics and 2D morphological variables of the bonnethead and scalloped hammerhead. We also examined the second moment of area along the length of the body and over a size range of animals to determine if there were shape differences along the body of these species and if those changed over ontogeny. We found that both species swim with the same standardized velocity and Strouhal number but there was no correlation between two-dimensional morphology and swimming kinematics. However, the bonnethead has a dorso-ventrally compressed anterior trunk and undulates with greater amplitude whereas the scalloped hammerhead has a laterally compressed anterior trunk and undulates with lower amplitude. We propose that differences in cross-sectional trunk morphology account for interspecific differences in undulatory amplitude. We also found that for both species, undulatory frequency is significantly greater in the anterior body compared to all other body regions. We hypothesize that the bonnethead and scalloped hammerhead swim with a double oscillation system.

Introduction

Hammerhead sharks, (Sphyrnidae) are characterized by a laterally expanded head (cephalofoil) that varies greatly among species (Lim et al., 2010; Thomson and Simanek, 1977). The most basal hammerhead lineage, represented by the winghead shark (*Eusphyra blochii*), possesses a cephalofoil that is proportionally the largest and measures up to 50% of their total body length (Lim et al., 2010). In comparison, the bonnethead shark (*Sphyrna tiburo*) is the most recently derived species and their cephalofoil width is 18% of total body length. Generally, as cephalofoil width increases among species, pectoral fin area decreases (Thomson and Simanek, 1977). Previous studies on hammerhead sharks focus primarily on cephalofoil morphology and its effects on hydrodynamics and sensory efficiency; however, little is known about the morphology and function of the post-cranial body. The significant morphological variation and the close phylogenetic relationship among hammerheads make them an ideal study system to examine the effects of shape on swimming performance.

Morphological differences in the body axis and caudal fin are known to affect swimming style in sharks (Flammang, 2014; Lindsey, 1979; Long and Nipper, 1996; Webb and Keyes, 1982). Stiff bodied species tend to displace their nearly homocercal caudal fin whereas flexible bodied sharks originate undulation anterior to their heterocercal tails (Donley et al., 2005; Lindsey, 1979; Long and Nipper, 1996; Webb and Keyes, 1982). Stiff bodied swimmers also undulate using smaller lateral displacements, encounter less incurred drag, and tend to be less maneuverable than their flexible bodied counterparts (Alexander, 2003; Webb and Keyes, 1982). Previous studies show that scalloped hammerheads have significantly smaller body stiffness and are more flexible than a non-hammerhead species; however, these comparisons have not been made among hammerheads (Kajiura et al., 2003). Given the influence of body shape on

swimming, our goal was to examine the effects of morphology on undulatory kinematics in two closely related hammerhead species.

Morphological variables such as body flexural stiffness, body profile, and caudal fin shape are known to affect fluid movement around the body and the shape of the vortex wakes produced during swimming (Long and Nipper, 1996; Webb and Keyes, 1982). To produce forward movement, sharks must generate an undulatory wave that reaches maximum amplitude at the caudal fin, shedding a wake of water that results in forward thrust (Alexander, 2003; Ferry and Lauder, 1996; Flammang et. al., 2011; Lindsey, 1979; Webb and Keyes, 1982; Wilga and Lauder, 2002). Fishes modulate this undulatory wave by changing the frequency and amplitude of lateral displacement (Hunter and Zweifel, 1971; Long et al., 2010). Increasing frequency, specifically tail beat frequency, is correlated with increasing swimming velocity, but the relation between amplitude and velocity is less well understood (Lauder et al., 2016; Sfakiotakis et al., 1999). Changes in frequency and amplitude also affect Strouhal number, which describes the cyclical motion of undulatory swimming (Alexander, 2003).

Undulatory reconfiguration, or changes in body shape during a tailbeat, can be observed when frequency and amplitude are determined along the length of the body, where the traveling wave is present during forward swimming (Long et al., 2010). Previous studies on hammerheads show that the amplitude of head yaw increases with cephalofoil size, but body frequencies and amplitudes have not been documented (McComb et al., 2009). The goals of the present study were to: (1) quantify variations in anterior trunk morphology (fineness ratio and second moment of area) between two species of hammerhead shark, the bonnethead (*Sphyrna tiburo*) and scalloped hammerhead (*Sphyrna lewini*); (2) compare the undulatory kinematics during volitional swimming; and (3) examine the relationship among morphological variables and

swimming kinematics in these two species. Firstly, we hypothesized that anterior body morphology varied such that species with larger heads have smaller pectoral fins (Thomson and Simanek, 1977). We also predicted that bonnethead anterior trunk stiffness, as measured by second moment of area and the anterior trunk fineness ratio, is intermediate to the values previously reported for scalloped hammerheads and sandbar sharks (*Carcharhinus plumbeus*), and the anterior body fineness ratio is positively correlated with head width (Kajiura et al., 2003). Secondly, we hypothesized that the scalloped hammerhead undulates at higher amplitude than the bonnethead based on previous studies demonstrating this trend in head yaw (McComb et al., 2009). We also predicted that both species have a higher undulatory frequency in the anterior body compared to the rest of the body. Finally, we hypothesized that within each species, morphological variables correlate with swimming kinematics. We predicted that cephalofoil area is negatively correlated with anterior body amplitude, anterior body fineness ratio is positively correlated with anterior body amplitude, and pectoral fin area is negatively correlated with mid-body amplitude.

Materials and methods

Study animals

Volitional swimming of scalloped hammerhead sharks, *Sphyrna lewini*, was filmed at the Hawaii Institute of Marine Biology as part of an approved IACUC protocol to T. C. Tricas at the University of Hawaii at Manoa. Young of the year scalloped hammerhead sharks (mean total length: 60.0 cm; n=4) were caught using hook and line from Kaneohe Bay, Oahu, HI, USA. Animals were housed and filmed together in a twelve-foot diameter tank at the Hawaii Institute of Marine Biology after a 24hr acclimation period. Individuals of the same species were filmed

together and distinguished by anatomical differences such as total length. Bonnethead sharks, *Sphyrna tiburo*, were collected in Long Key, FL, USA, and cared for under an approved IACUC protocol granted to the authors. Sub-adult to adult bonnethead sharks (mean total length: 89.2 cm; n=4) were caught in shallow waters using a gill net near Long Key, FL. Animals were housed and filmed in a sixteen-foot diameter tank at the Florida Atlantic University Marine Research Facility, FL, USA. Bonnetheads acclimated for 24hrs prior to swimming trials and were filmed one individual at a time.

In this study, bonnethead and scalloped hammerhead sharks are in different life history stages, but they are approximately matched for body size. Adult scalloped hammerheads mature between 140cm TL (males) and 212 cm TL (females) and pose many captivity and husbandry challenges in a lab setting (Compagno, 1984). As a result of varying life history, there may be ontogenetic differences not captured in these data. We attempted to mitigate these differences by using data standardized by total length for swimming velocity and tail beat amplitudes, and size independent variables like flexion frequency (Hz) and flexion amplitude (^{o}).

Morphological measurements

For each shark, we captured still images from video footage and measured the whole *dorsal body area* (cm^2) using ImageJ (1.38X available from the National Institutes of Health). We partitioned out the *cephalofoil area* and total *pectoral fin area*, which were standardized by *dorsal body area*. *Total planning area* was calculated as the sum of the *cephalofoil area* and *pectoral fin area* and was standardized by *dorsal body area.* To make direct comparisons with published data, we also quantified *cephalofoil width* (cm) as measured from eye to eye (McComb et al, 2009; Thomson and Simanek, 1977). We measured the *anterior body fineness*

ratio defined as the maximum width divided by the length of the anterior trunk region from the base of the cephalofoil to the origin of the pectoral fins.

To examine cross-sectional morphology of the anterior trunk, we CT scanned a bonnethead (n=1, TL = 68.83cm) and scalloped hammerhead (n=1, TL = 51.94cm) shark on a GE Medical Systems LightSpeed 16 CT scanner with 0.625mm slice thickness at South Florida Radiation Oncology. Single slice images (512x512p) from the scans were used to calculate the *second moment of area* (*I*), a structural predictor of stiffness, at multiple points along the body as determined by individual slices at those landmarks. *Second moment of area* (*I*) was measured at five anatomical landmarks along the total length: (A) base of the cephalofoil, (B) third gill slit, (C) anterior pelvic fin origin, (D) anterior origin of the second dorsal fin, (E) and caudal peduncle. *I* was calculated in both the dorso-ventral ($I_y = \pi \frac{ab^3}{4}$) and lateral ($I_x = \pi \frac{a^3 b}{4}$) orientations. The ratio of these measurements was used to compare cross-sectional shape between the two specimens to remove the effect of body size (Mulvany and Motta, 2013). To investigate the effect of ontogeny on anterior body shape, a cross-section at the third gill slit (region B) was dissected from fresh frozen individuals of varied body length for the scalloped hammerhead (n=4, TL=51.9cm - 250cm) and the bonnethead (n=10, TL=14.6cm - 96.5cm). Cross-sections were scaled with a 15cm ruler and photographed with a Nikon D3300 for ImageJ analysis and *I* was calculated as outlined above. A simple linear regression of I_x:I_y vs. *total length* (cm) was used to determine if there were differences in shape through ontogeny.

Kinematic analysis

Video was filmed from a dorsal view with a GoPro Hero3 at 30 fps and 1080x1920p as the sharks swam volitionally. A flat port housing was used and the cameras were set to narrow field of view to eliminate the barrel distortion of GoPro cameras. Sharks occupied less than 5% of the frame and we selected trials in which individuals were centered in the frame to avoid potential distortions at the edges of the field of view. Cameras were mounted 1m above the water surface and water depth was approximately 1m. Variables were standardized to animal total length or variables were size independent (units of Hz or º) to minimize effects of varying sizes among individuals and depth of each swim in the tank. A 30cm ruler was placed at the bottom of the tank to provide scale for the camera. To ensure that the same trials were not analyzed twice, video was analyzed sequentially to select clips in which sharks completed at least three full tail beat cycles of straight, steady swimming.

We analyzed eight anatomical landmarks using LoggerPro 3.10.1 point tracking software (Vernier Software & Technology, Beaverton, OR, USA; Fig. 1). Anatomical landmarks included: (A) the tip of the rostrum, (B) midline at the gills, (C) anterior origin of the first dorsal fin, (D) anterior origin of the second dorsal fin, (E) caudal peduncle, (F) tip of the caudal fin, (G) left posterior margin of the cephalofoil, and (H) right posterior margin of the cephalofoil (Fig. 1). To account for noise, point tracking data were filtered using a low-pass, fourth order butterworth filter at 5Hz (Erer, 2007).

We measured variables related to the overall swimming performance. We calculated *velocity* (*V;* $cm \cdot s^{-1}$) by measuring the displacement of point C from frame to frame over the time between frames. This was averaged over the duration of the clip (at least three tail beats). A tail

beat cycle is defined as the excursion of the tail from peak lateral flexion on one side back to peak lateral flexion on the same side. We measured *tail beat frequency* (*f*; Hz) for each clip as cycles per second. *Tail beat amplitude* (*A*; cm) was measured as the peak-to-peak distance covered by the tail from full lateral flexion on one side to the full lateral flexion on the other. We then calculated *Strouhal number* (*St*) as

$$St = \frac{Af}{V}$$

where *A* is peak-to-peak *tail beat amplitude* (cm), *f* is *tail beat frequency* (Hz), and *V* is *velocity* (cm·s^{-1}) (Rohr and Fish, 2004). To remove the effect of body size when comparing between species, both *tail beat amplitude* (*St. A*) and *velocity* (*U;* body lengths·s^{-1}) were standardized by total length.

Regional flexion and amplitude were measured for the anterior body (AB) as angular displacement of the anterior trunk (point B); for the mid-body (MB) as angular displacement at the dorsal fin origin (point C); for the posterior body (PB) as angular displacement at the second dorsal fin origin (point D); and for the caudal fin (CF) as angular displacement at the caudal peduncle (point E) (Fig. 1). *Flexion amplitude* was measured as the maximum displaced angle from the straightened midline (180^{o}) and *flexion frequency* was calculated as the maximum displacement per time averaged over at least three tail beats. The anterior body (AB) flexion frequency is synonymous with head yaw quantified in previous studies (McComb et al., 2009).

Statistical analysis

For both species, video was obtained for four individuals. We selected a maximum of three clips per individual to maintain a balanced design. For each variable, we calculated the mean for each shark and we used those mean values for statistical analyses. Each variable was

evaluated to ensure normality and homoscedasticity using a Shapiro-wilk test, and variances were analyzed using ANOVA with JMP v.5.0.1.a (SAS Institute Inc., Cary, NC, USA). The *flexion frequency* and *flexion amplitude* were analyzed using mixed-effects ANOVA with species, region, and the interaction term as fixed effects and individual was coded as a random effect. Post-hoc t-tests were used to compare the means of each species at each region, using a standard Bonferroni corrected alpha value of P = 0.0125. Linear regressions analyses were used to assess the relations of kinematic variables with the morphological variables outline above.

Results

Morphology

*Total leng*th (*TL*) and *dorsal body area* were significantly different between species ($F_{1,6}$ = 67.7894, P = 0.0002; $F_{1,6}$ = 53.0927, P = 0.0003; respectively; Supplemental Table 1). To account for size and body area differences when comparing between species, we standardized *cephalofoil and pectoral fin area* by *dorsal body area*. As predicted, *standardized cephalofoil area* was significantly greater in the scalloped hammerhead whereas standardized *pectoral fin area* was significantly higher in the bonnethead (Fig. 2A,B; $F_{1,6}$ = 51.4146, P = 0.0004; $F_{1,6}$ = 76.3849, P < 0.0001). When considering the total area of the planing surface (*cephalofoil area* + *pectoral fin area*), we found that the *standardized planing area* was significantly greater in the scalloped hammerhead (Fig 2C; $F_{1,6}$ = 18.4857, P = 0.0051). Additionally, the *anterior body fineness ratio* was significantly higher in the scalloped hammerhead (Fig. 2D; $F_{1,6}$ = 63.2371, P = 0.0002).

For all five regions of the body axis, *second moment of area* (*I*) was greater in the bonnethead (Fig. 3A). To remove the effect of body size, we calculated the ratio of *second moment of area* (*I*) measured in the dorsal-ventral direction (I_y) to *second moment of area* measured in the lateral direction (I_x) as a quantification of shape (Mulvany and Motta, 2013). A ratio of one indicates a perfect circle, greater than one indicates lateral body compression, and less than one indicates dorso-ventral body compression. For four of the five cross sectional body regions, the scalloped hammerhead had a greater I_x:I_y ratio (Fig. 3B). Additionally, the greatest differences in cross-sectional shape between species were in the first two cross-sections at the base of the cephalofoil and third gill slit (the anterior trunk region).

To ensure the variations in anterior body cross-sectional morphology reported in Fig. 2 were not an effect of total body length (a proxy for ontogeny in each species), we examined the I_x:I_y ratio at the third gill slit among animals of varying size in the scalloped hammerhead (n=4, TL 51.9cm – 250cm) and the bonnethead (n=10, TL 18.5cm – 111.5cm) (Fig. 4A). There was no significant difference in the cross-sectional shape for either species across total length; however, I_x:I_y was significantly greater in the scalloped hammerhead (Fig. 4B: $F_{1,12} = 13.4256$, P= 0.0032).

Kinematics

Neither *velocity* ($m \cdot s^{-1}$) nor *standardized velocity* (body lengths$\cdot s^{-1}$) was different between species (Fig. 5A; Supplemental Table 2; P = 0.1712 and P = 0..2334, respectively). *Strouhal number* was not different between species (Fig. 5B; Supplemental Table 2; P = 0.2180). Neither

tail beat frequency nor *standardized tail beat amplitude* differed between species (Fig. 5C and D; P = 0.2072 and P = 0.8199; respectively).

A mixed effects ANOVA showed that flexion amplitude was significant with species and region as fixed effects and individual as a random effect (Fig. 6A; $R^2 = 0.9496$, $P < 0.0001$). Flexion amplitude was significantly greater in the bonnethead with species as a fixed effect ($F_{1,6} = 9.7661$ P=0.0205). Region was also a significant fixed effect ($F_{3,18} = 114.356$, $P < 0.0001$). Post-hoc comparisons show that *flexion amplitude* in both species was lowest in the anterior body (AB), greatest at the caudal fin (CF), and the mid-body (MB) and posterior body (PB) were intermediate and not significantly different from one another. Between species, there was no difference in *flexion amplitude* in the CF; however, AB, MB and PB amplitude were significantly greater in the bonnethead (P = 0.0141, P = 0.0159, P = 0.0057; respectively).

Flexion frequency was also significant as a mixed effects ANOVA with species, and region as fixed effects and individual as a random effect (Fig 6B; $R^2 = 0.8899$, $P <0.0001$). Region was the only significant effect ($F_{3,18} = 2.2007$, $P < 0.0001$). Post-hoc analyses show that for both species, *flexion frequency* was greatest in the AB and there was no significant difference among the MB, PB, and CF ($P < 0.0001$).

We used simple linear regressions to examine the effects of morphology on *flexion amplitude*, which was the only kinematic variable different between species. For both species, there was no relation between *anterior body fineness ratio* and *anterior body amplitude*, contrary to our predictions. There was also no relation between *standardized cephalofoil area* and AB *flexion amplitude*. Finally, MB *flexion amplitude* was not correlated with *pectoral fin area*.

Discussion

Previous studies have demonstrated that closely related bonnethead (*Sphyrna tiburo*) and scalloped hammerhead (*Sphyrna lewini*) sharks differ in morphology, sensory physiology, body flexibility, and head yaw amplitude; however, there are limited data on the effect of morphology on swimming kinematics in these two species (Kajiura et al., 2003; Lim et al., 2010; Mara et al., 2015; Mccomb et al., 2009; Thomson and Simanek, 1977). Our goal was to link morphological variation between species with differences in swimming kinematics. In addition to differences noted in previous studies (cephalofoil width, pectoral fin area), we showed whole body variation in morphological variables between these species (cephalofoil area, pectoral fin area, dorsal body area, anterior fineness ratio, second moment of area; Figs 2-4). Despite having different morphologies, the swimming kinematics of these species was similar (Fig 5). We were not able to show any correlations among these morphological variables and kinematics within each species. However, we found that these species employ different undulatory strategies to produce similar *standardized velocity* (body lengths$\cdot s^{-1}$) and *Strouhal number* (Fig. 6). The scalloped hammerhead has a larger cephalofoil, narrower anterior trunk, and swims at a low undulatory amplitude whereas the bonnethead has a smaller cephalofoil, wider anterior trunk, and swims at a higher amplitude.

Morphological Variation

Bonnethead and scalloped hammerhead sharks show large variations in external morphology. We supported our hypothesis that the bonnethead has a proportionally smaller cephalofoil and larger pectoral fin area whereas the scalloped hammerhead had a proportionally

larger cephalofoil and smaller pectoral fin area (Fig. 2). A similar inverse relation between the cephalofoil and pectoral fin area has also been noted in the smooth hammerhead (*Sphyrna zygaena*) (Thomson and Simanek, 1977). Previous data show the inverse relation between pectoral fin area and cephalofoil area results in the same total area of planning surfaces in the bonnethead, scalloped hammerhead, and smooth hammerhead; however, we found that the scalloped hammerhead has a significantly larger planning surface area than the bonnethead (Thomson and Simanek, 1977). These data also support our hypothesis that the *anterior body fineness ratio* of the scalloped hammerhead shark was significantly greater than the bonnethead, demonstrating that the scalloped hammerhead has a narrower anterior trunk (Fig. 2D).

We predicted that the bonnethead would have an anterior trunk that is stiffer than the scalloped hammerhead but not as stiff as the sandbar shark. We found that the anterior body (AB) *second moment of area* (I_x) of the bonnethead is greater than the scalloped hammerhead, suggesting that the bonnethead anterior body is structurally stiffer (Fig. 3A; Kajiura et al., 2003). However, the *second moment of area* measurements we found are greater than values previously reported for the scalloped hammerhead due to overall differences in body size, and we are unable to compare our I_x results to those reported for a non-hammerhead species (Kajiura et al., 2003). To account for the differences in body size between the bonnetheads and scalloped hammerheads in this study, we compared the cross-sectional trunk shape quantified as the ratio I_x:I_y, where values greater than one indicate lateral compression and less than one indicate dorso-ventral compression. The greater I_x:I_y ratios at four of the five cross-sectional regions further suggest that the trunk of the scalloped hammerheads is laterally compressed and likely more flexible than the bonnethead (Fig. 3B). The bonnethead has significantly more dorso-ventrally compressed anterior trunk and is probably stiffer than the scalloped hammerhead (Fig. 3B). We also

demonstrated that across ontogeny, there is no change in anterior trunk shape in both species, and the bonnethead has a significantly more dorso-ventrally compressed anterior trunk and is likely stiffer than the scalloped hammerhead (Fig. 4)

Undulatory Variation

In addition to differences in trunk cross-sectional morphology and stiffness, we found that bonnethead and scalloped hammerhead sharks modulate the frequency and amplitude of the undulatory wave to produce overall similar kinematic outputs. *Standardized velocity* (*U*), *Strouhal number* (*St*), *tailbeat frequency* (*f*), and *standardized tail beat amplitude* (*St. A*) were statistically similar between species (Fig. 5). Based on previous studies showing that the scalloped hammerhead has a greater amplitude of head yaw, we hypothesized that the scalloped hammerhead would have a greater undulatory amplitude at all body regions compared to the bonnethead. We found differences in regional *flexion amplitude* between species; however, the mid-body and posterior body were significantly more displaced in the bonnethead rather than the scalloped hammerhead as predicted (Fig. 6A). We suggest that differences in mid-body amplitude may be a result of differing cross-sectional trunk morphology; however, we were not able to directly test this relation with our data, as we were unable to obtain cross-sectional data from the sharks used in the kinematic analyses.

We supported our hypothesis that the anterior body undulates at a higher frequency than the rest of the body in both species (Fig. 6B). The white sturgeon, *Acipenser transmontanus*, swims using a double oscillating system, where undulatory frequency in the anterior body differs from the rest of the body (Fig. 6B; Long, 1995). These complexities in undulatory wave propagation have also been observed in lamprey and eel, and they may stand apart from the

traditional ridged bodied teleost model where undulatory amplitude increases rostro-caudally (Long, 1995; Root et al., 1999; Long et al., 2010). With the exception of the eel, these patterns have been observed in fishes with cartilaginous vertebral columns or notochords, and are perhaps due to the mechanical properties of cartilaginous fishes (Porter et al., 2014; Porter et al., 2016; Long et al., 2004; Long et al., 2002). It has been suggested that anterior body flexion may be a result of recoil from body undulation, or that it may control the driving frequency of undulation; however, recent studies show that movement of fishes heads increases their sensitivity to external stimuli (McHenry et al., 1995; Webb, 1988, Akanyeti et al., 2016). Additionally, fish may have morphological adaptations associated with damping or selectively alter damping coefficients to minimize the effect recoil and higher order harmonics (Lighthill, 1977; Long, 1988; Root *et al*., 1999; Webb, 1988). We suggest that bonnethead and scalloped hammerhead sharks increase anterior body frequency independently from the rest of the body to increase sensory perception (i.e., electroreception and vision) (Kajiura and Holland, 2002; McComb et al., 2009). Increased anterior body frequency (yaw defined in McComb et al., 2009) is particularly important for the bonnethead and scalloped hammerhead because it increases the area covered by the cephalofoil when scanning for bioelectric fields, a critical hunting behavior in benthic animals (Kajiura, 2001; Kajiura and Holland, 2002). Furthermore, head yaw increases the visual binocular overlap by upwards of 15^{o} in both species (McComb et al., 2009). The greater anterior body *flexion frequency* for both species may allow bonnethead and scalloped hammerhead sharks to increase sensory perception without increasing whole-body frequency and the associated energetic cost (Fig. 6B). Finally, the double oscillation system shown here, in which the anterior body undulates at a different frequency than the posterior body, may be specific to cartilaginous fishes (Long, 1995). Shark vertebral columns are non-linear, viscoeleastic systems that store and

transmit energy behaving as both a spring and a brake, which allows for the differential transmission of power depending on the undulatory amplitude and frequency (Porter et al., 2016; Porter et al., 2014). We hypothesize that the variable mechanical behavior of the cartilaginous vertebral column allows for high frequency undulation in the anterior body without disrupting lower frequency, posterior body undulation.

Finally, we did not support our hypothesis that morphological variables would correlate with swimming kinematics within each species. We found no relation between cephalofoil area and anterior body amplitude, anterior body fineness ratio and anterior body amplitude, or pectoral fin are and mid body amplitude. These results may be due to the high variability associated with volitional swimming kinematics and narrow range of morphological variability within our individuals. Future studies may examine the relation of morphological variables and swimming kinematics of hammerhead shark where differences may be evident when examining more species or a greater variation in sizes.

We show that bonnethead and scalloped hammerhead morphology varies along the length of the whole body dorsally and in cross-section (Fig. 2-4). We propose that the differences in undulatory amplitude observed between these species are a result of trunk stiffness (as measured by *second moment of area* and *anterior body fineness ratio)* and *cephalofoil width* (Fig. 2-4). We were not able to correlate any of the 2D morphological variables examined here with swimming kinematic outputs. We hypothesize that the dorso-ventrally compressed anterior trunk of the bonnethead may be more resistant to high frequency bending and rather compensates with high amplitude undulation. Future studies should focus on examining the relation between second moment of area variations along the body with differences in flexion amplitude and frequency.

Conclusions

Previous literature focuses primarily on morphology and function of the cephalofoil of hammerhead sharks. This is the first study to examine whole body morphology and swimming kinematics of two hammerhead species. We found that morphologically different scalloped hammerhead and bonnethead sharks swim at similar volitional velocities and Strouhal numbers, but modulate the amplitude of undulation differently. The scalloped hammerhead has a larger cephalofoil, laterally compressed anterior trunk, and undulates at a lower flexion amplitude in comparison the bonnethead which has a smaller cephalofoil and dorso-ventrally compressed anterior trunk. We found that both species exhibit greater flexion frequency in the anterior body setting up a double oscillating system, which we propose may be specific to fishes with cartilaginous skeletons. We hypothesize that high frequency head yaw increases sensory perception without the added energetic costs increasing undulatory frequency throughout the whole body.

Acknowledgements. We thank M. E. Bowers, S. C. Leigh, and the Keys Marine Laboratory for assistance in collection and husbandry of bonnethead sharks. We thank T. C. Tricas for video of the volitional swimming of hammerhead sharks at the Hawaii Institute of Marine Biology. We thank R. Sanders and R. McConkey assistance digitizing video clips. We thank Mote Marine lab for collecting a bonnethead and scalloped hammerhead specimens for CT scanning under FWC-SAL-13-0041-SRP, and T. Leventouri, S. Pella, and T. L. Meredith for CT scanning time. We thank L. J. Natanson and D. Adams for collection of fresh frozen scalloped hammerhead and bonnethead specimens. S. M. Kajiura, P. J. Motta, and J. H. Long Jr. also provided thoughtful advice throughout this project and on the manuscript. This manuscript has been greatly improved due to the comments from three anonymous reviewers.

Competing interests. The authors declare that they have no competing interests.

Author's contributions. All authors contributed to video and data analysis. M.E.P. and S.L.H. prepared the manuscript and all authors contributed to the final version. All authors read and approved the final manuscript.

Funding. This research was supported by the United States National Science Foundation (IOS-649 0922605) and Florida Atlantic University startup funds to M.E.P.

Data accessibility. All data used are available on dataverse doi:10.7910/DVN/KNTDKZ

References

Akanyeti, O., Thornycroft, P. J. M., Lauder, G. V., Yanagitsuru, Y. R., Peterson, A. N., Liao, J. C. (2016). Fish optimize sensing and respiration during undulatory swimming. Nat. Commun. 7.

Alexander, R. M. (2003). Principles of Animal Locomotion. Princeton, NJ: Princeton University Press.

Anderson, J. M., Streitlien, K., Barrett, D. S. and Triantafyllou, M. S. (1998). Oscillating foils of high propulsive efficiency. J. Fluid Mech. 360, 41–72.

Compagno, L. J. V. (1984). FAO Species Catalogue, vol. 4, Sharks of the World. Rome: Food and Agricultural Organization of the United Nations.

Donley, J. M., Shadwick, R. E., Sepulveda, C. A, Konstantinidis, P. and Gemballa, S. (2005). Patterns of red muscle strain/activation and body kinematics during steady swimming in a lamnid shark, the shortfin mako (Isurus oxyrinchus). J. Exp. Biol. 208, 2377–2387.

Erer, K. S. (2007). Adaptive usage of the butterworth digital filter. J. Biomech. 40, 2934-2943.

Flammang, B. E. (2014). The fish tail as a derivation from axial musculoskeletal anatomy: An integrative analysis of functional morphology. Zoology 117, 86–92.

Hunter, J. R. and Zweifel, J. R. (1971). Swimming speed, tail beat frequency, tail beat amplitude, and size in jack mackerel, Trachurus symmetricus, and other fish. Fish. Bull. 69, 253–266.

Kajiura, S. M. (2001). Head morphology and electrosensory pore distribution of carcharhinid and sphyrnid sharks. 125–133.

Kajiura, S. M. and Holland, K. N. (2002) Electroreception in juvenile scalloped hammerhead and sandbar sharks. J. Exp. Biol. 205, 3609-3621.

Kajiura, S. M., Forni, J. B. and Summers, A. P. (2003). Maneuvering in juvenile carcharhinid and sphyrnid sharks: the role of the hammerhead shark cephalofoil. Zoology 106, 19–28.

Lauder, G. V., Anderson, E. J., Garborg, C. S., Thornycroft, P., Turner, E., Kalionzes, K. and Kenaley, C. P. (2016). Revisiting the relationship between tail beat frequency, amplitude, and speed in swimming fishes. In Society for Integrative and Comparative Biology Meeting, p. Portland, OR.

Lighthill, M. J. (1977). Mathematical theories of fish swimming. In Fisheries Mathematics (ed. Steele, J. H.), pp. 131–144. New York: Academic Press.

Lim, D. D., Motta, P., Mara, K. and Martin, A. P. (2010). Phylogeny of hammerhead sharks (Family Sphyrnidae) inferred from mitochondrial and nuclear genes. Mol. Phylogenet. Evol. 55, 572–579.

Lindsey, C. C. (1979). Form, Function, and Locomotory Habits in Fish. Fish Physiol. 7, 1–100.

Long, J. H. (1988). Muscles, elastic energy, and the dynamics of body stiffness in swimming eels. Am. Zool. 38, 771–792.

Long, J. H. (1995). Morphology, mechanics, and locomotion: the relation between the notochord and swimming motions in sturgeon. Environ. Biol. Fishes. 199–211.

Long, J. H., Koob-Emunds, M., Sinwell, B. and Koob, T. J. (2002). The notochord of hagfish, Myxine glutinosa: viscoelastic properties and mechanical functions during steady swimming. J. Exp. Biol. 205, 3819-3831.

Long, J. H., Koob-Emunds, M. and Koob, T. J. (2004). The mechanical consequences of vertebral centra. The Bulletin, Mount Desert Island Biological Laboratory. 43, 99-101.

Long, J. H., Porter, M. E., Root, R. G. and Liew, C. W. (2010). Go reconfigure: How fish change shape as they swim and evolve. Integr. Comp. Biol. 50, 1120–1139.

Long, J. H. and Nipper, K. S. (1996). The importance of body stiffness in undulatory propulsion. Am. Zool. 36, 678–694.

Mara, K. R., Motta, P. J., Martin, A. P. and Hueter, R. E. (2015). Constructional morphology within the head of hammerhead sharks (sphyrnidae). J. Morphol. 0, n/a-n/a.

Mccomb, D. M., Tricas, T. C. and Kajiura, S. M. (2009). Enhanced visual fields in hammerhead sharks. 4010–4018.

Mchenry, M., Pell, C. and John, J. H. (1995). Mechanical control of swimming speed: stiffness and axial wave form in undulating fish models. J. Exp. Biol. 198, 2293–305.

Mulvany, S. and Motta, P. J. (2013). The morphology of the cephalic lobes and anterior pectoral fins in six species of batoids. J. Morphol. 274, 1070–1083.

Nakaya, K. (1995). Hydrodynamic Function of the Head in the Hammerhead Sharks (Elasmobranchii: Sphyrnidae). Copeia 1995, 330–336.

Porter, M. E., Ewoldt, R. H. and Long, J. H., (2016). Automatic control: the vertebral column of dogfish sharks behaves as a continuously variable transmission with smoothly shifting functions. J. Exp. Biol. 219, 2908-2919.

Rohr, J. J., Fish, F. E. (2004). Strouhal numbers and optimization of swimming by odontocete cetaceans. J. Exp. Biol. 207, 1633–1642.

Root, R. G., Courland, H. W., Pell, C. A., Hobson, B., Twohig, E. J., Suter, R. B., Shepherd, W. R., Boetticher, N. C. and Long, J. H. (1999). Swimming fish and fish-like models: The harmonic structure of undulatory waves suggests that fish actively tune their bodies. Proc. 11th Int. Symp. Unmanned Untethered Submers. Technol. 378–388.

Root R. G., Courtland H. W., Shepherd W, and Long, J. H. (2007). Flapping flexible fish: periodic and secular body reconfigurations in swimming lamprey, Petromyzon marinus. Exp Fluids. 43:779–97.

Sfakiotakis, M., Lane, D. M. and Davies, J. B. C. (1999). Review of fish swimming modes for aquatic locomotion. IEEE J. Ocean. Eng. 24, 237–252.

Thomson, K. S. and Simanek, D. E. (1977). Body form and locomotion in sharks. Integr. Comp. Biol. 17, 343–354.

Triantafyllou, M. S., Triantafyllou, G. S. and Yue, D. K. P. (2000). Hydrodynamics of Fishlike Swimming. 33–53.

Webb, P. W. (1988). “Steady” swimming kinematics of Tiger musky, an esociform accelerator, and rainbow trout, a generalist cruiser. J. Exp. Biol. 138, 51–69.

Webb, P. W. and Keyes, R. S. (1982). Swimming kinematics of sharks. Fish. Bull. 80, 803–812.

Figures

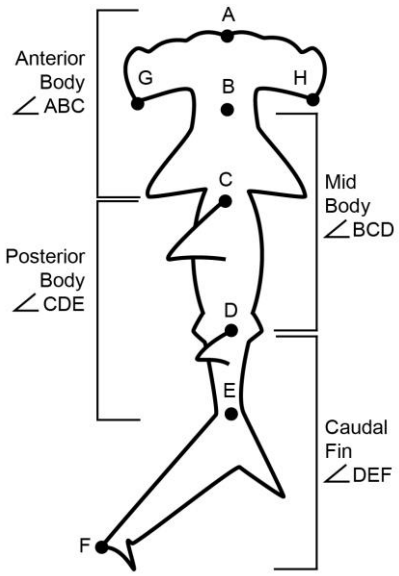

Fig. 1: Eight anatomical landmarks were digitized on each individual for both species. For regional flexion frequency and amplitude analyses, four isolated regions are outlined in brackets as the anterior body (angle ABC), mid-body (angle BCD), posterior-body (angle CDE), and caudal peduncle (angle DEF).

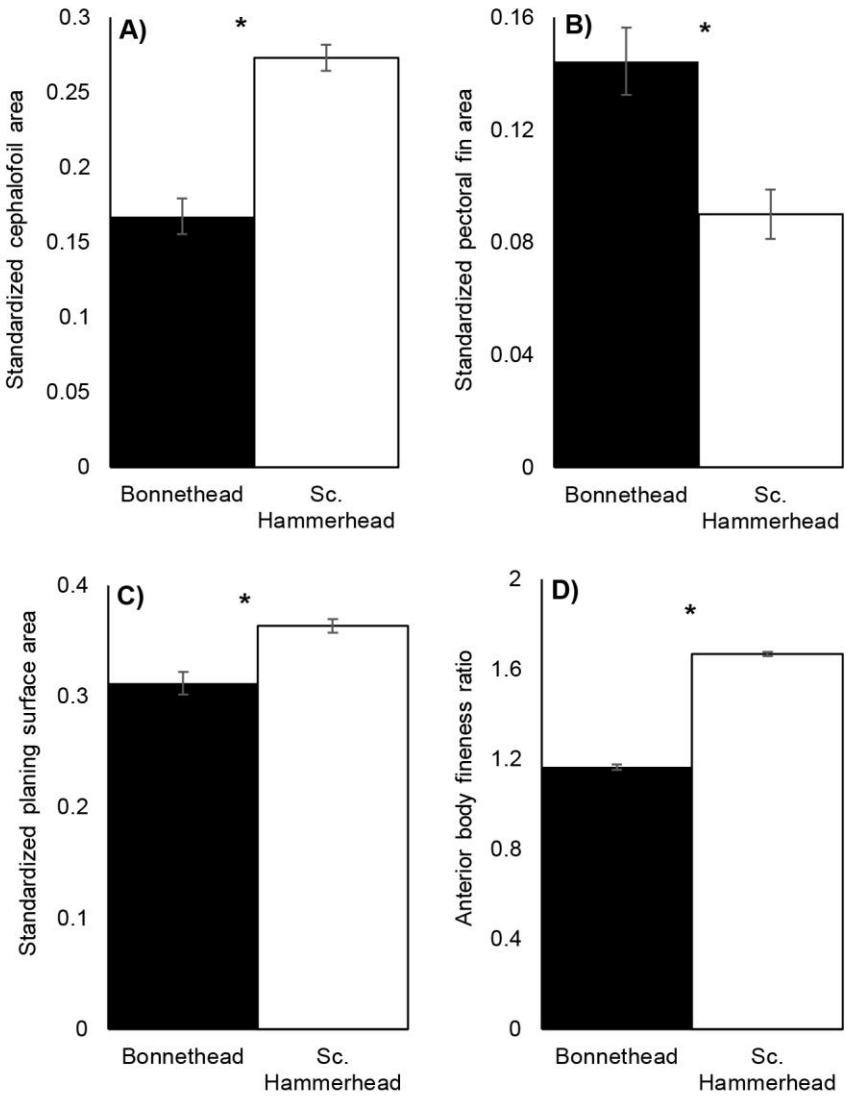

Fig. 2: Morphological differences between bonnethead (black) and scalloped hammerhead (white) bodies. (A) The cephalofoil (standardized by dorsal body area) of the scalloped hammerhead shark was 39% larger than the bonnethead though the standardized pectoral fin area (B) of the bonnethead was 38% larger. (C) Standardized planning surface area (cephalofoil area + pectoral fin area) of the scalloped hammerhead was 5% greater than the bonnethead. (D) Anterior body fineness ratio was 30% greater in the scalloped hammerhead. Error bars represent standard error. Stars denote significant statistical differences.

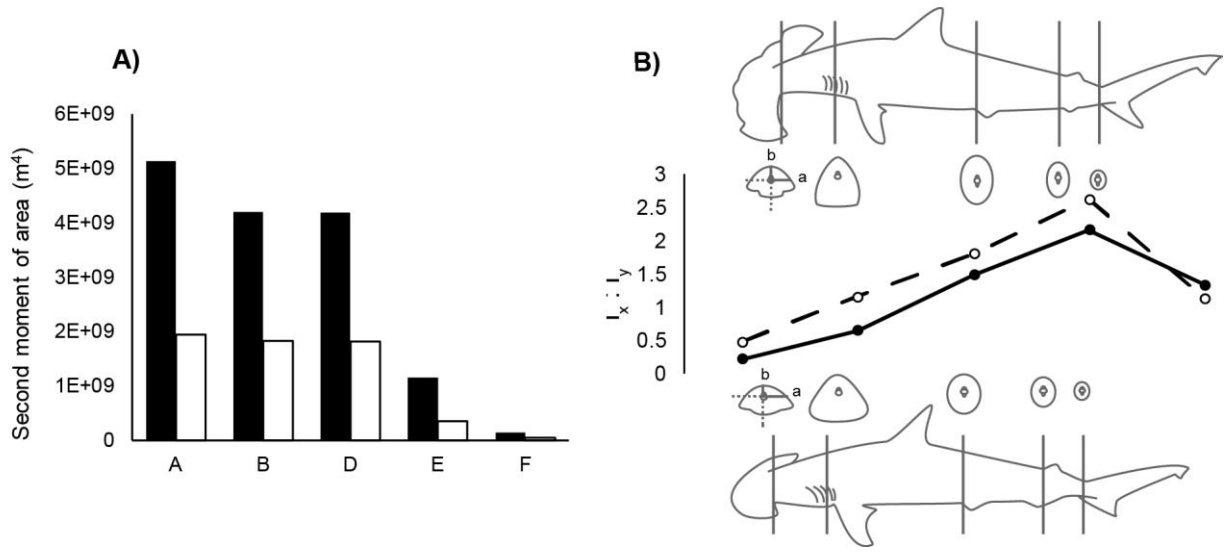

Fig. 3: Regional variation in second moment of area of the body between bonnethead (black) and scalloped hammerhead sharks (white). (A) Second moment of area (I_x) was greater in the bonnethead compared to the scalloped hammerhead at all five regions. (B) I_x:I_y was greater in the scalloped hammerhead at four of the five regions, demonstrating that the scalloped hammerhead has a more laterally compressed trunk. The biggest differences in shape between the two species was observed in the anterior trunk region.

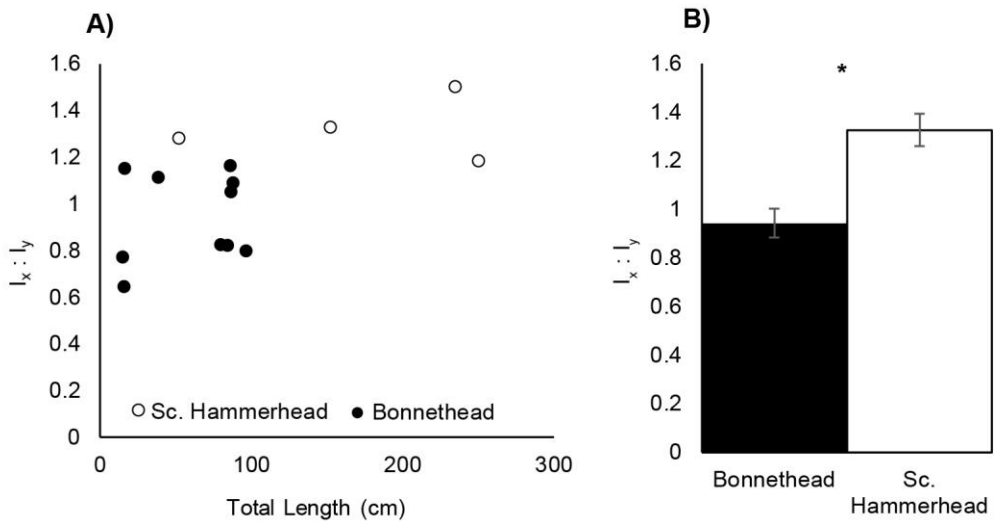

Fig. 4: Variations in anterior body cross-sectional morphology, quantified as $I_x:I_y$ at third gill slit. (A) There was no difference in cross sectional shape across body sizes for either species. (B) Cross sectional shape was approximately circular ($I_x:I_y = 1$) in the bonnethead in comparison to the scalloped hammerhead in which the body was laterally compressed ($I_x:I_y > 1$). Error bars represent standard error. Stars denote significance.

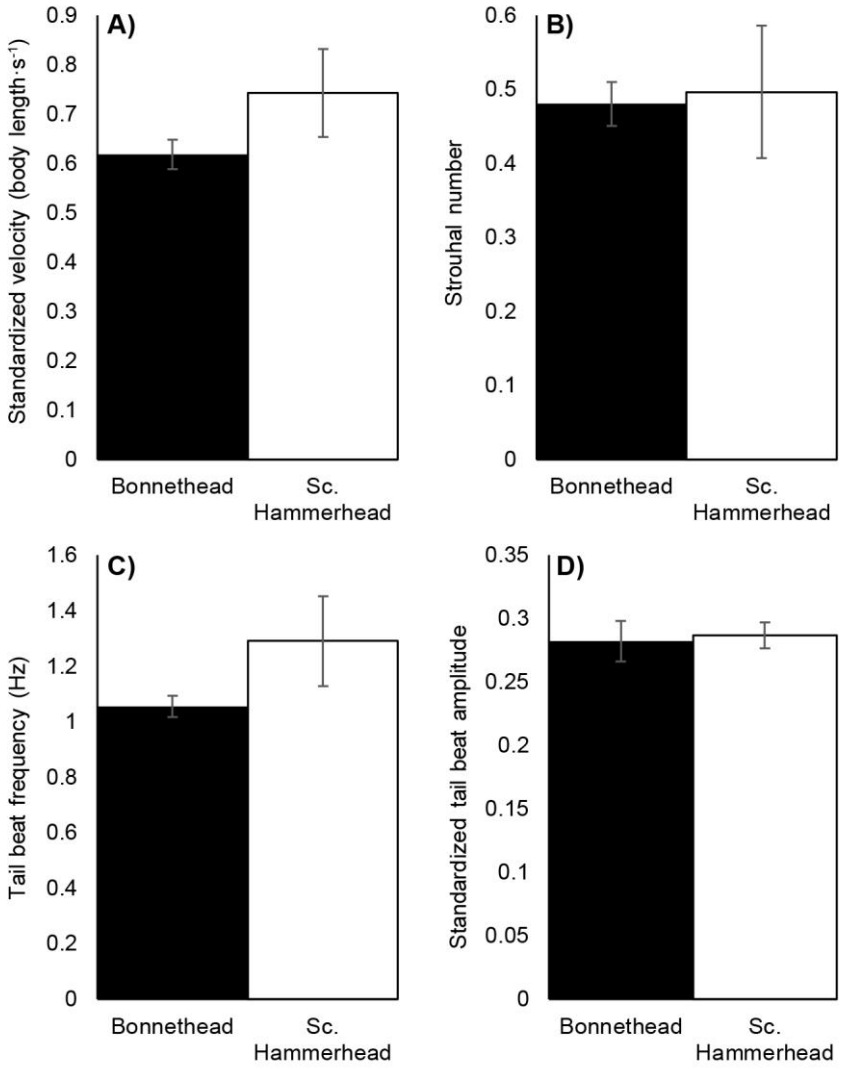

Fig. 5: Comparison of performance variables between the bonnethead (black) and scalloped hammerhead (white). (A, B) Neither velocity ($cm \cdot s^{-1}$) nor standardized velocity (body $lengths \cdot s^{-1}$) was significantly different between species. (C, D) Tail beat frequency and standardized tail beat amplitude did not vary between species. Error bars represent standard error.

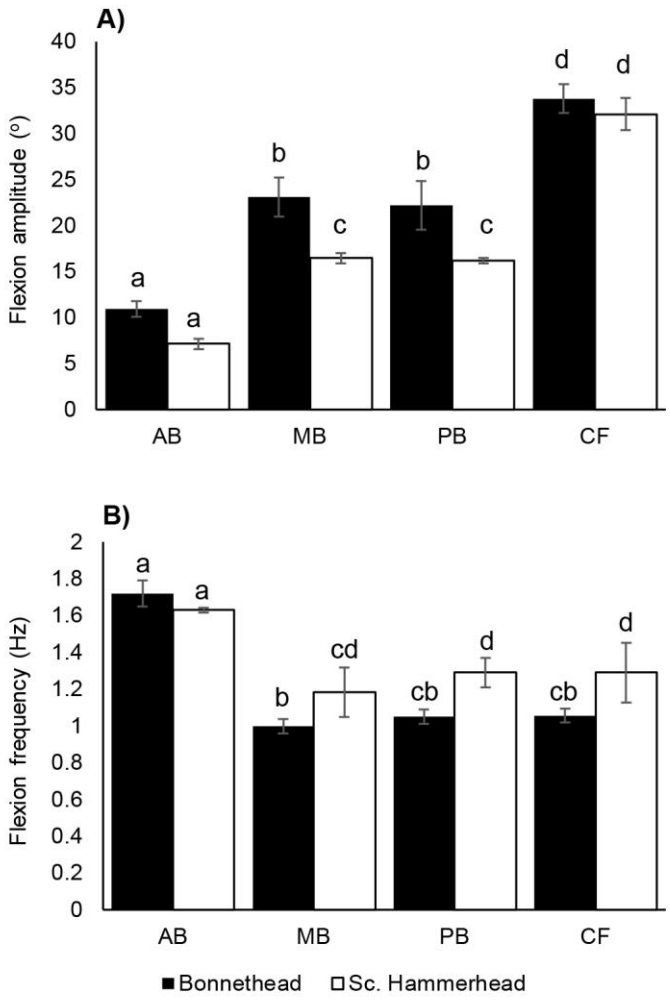

Fig. 6: Flexion variables differed between bonnethead (black) and scalloped hammerhead (white) sharks. (A) Midline amplitude increased significantly along the length of the body with the largest amplitudes produced in the caudal region. Midline amplitude differed between species at MB and PB regions where bonnethead amplitude was on average 28% greater than the scalloped hammerhead. (B) AB had significantly higher frequencies than the three posterior regions (MB, PB, CF) in both species and was not different between species. The frequency of flexion was consistent across the three posterior regions (MB, PB, CF) for both species. Error bars represent standard error. Lower case letters denote significant statistical differences.

Supplemental Table 1: Morphological measurements of bonnethead and scalloped hammerhead sharks ± standard error.

Species	*Total length (cm)	*Dorsal body area (cm^2)	*Cephalofoil width (cm)	*[1]Cephalofoil area	*[1]Pectoral fin area	[1]*Planing surface area	*Fineness ratio
Bonnethead	89.27 ± 3.11	590.41 ± 41.48	13.18 ± 0.52	0.17 ± 0.01	0.14 ± 0.003	0.31 ± 0.015	1.16 ± 0.03
Scalloped Hammerhead	59.96 ± 1.73	265.44 ± 16.39	15.23 ± 0.45	0.27 ± 0.01	0.09 ± 0.005	0.36 ± 0.01	1.66 ± 0.05

*Denote significant differences between species. [1]Due to the significant differences in total length (P = 0.0002) and dorsal body area (P = 0.0003), we standardized cephalofoil area, pectoral fin area, and planning surface area by the dorsal body area.

Supplemental Table 2: Performance variables for bonnethead and scalloped hammerhead sharks ± standard error.

Species	[1]Standardized velocity (body lengths · s^{-1})	Tail Beat Frequency (Hz)	[1]Tail Beat Amplitude	Strouhal number
Bonnethead	0.646 ± 0.040	1.056 ± 0.038	0.282 ± 0.016	0.481 ± 0.010
Scalloped Hammerhead	0.716 ± 0.043	1.291 ± 0.16	0.287 ± 0.010	0.497 ± 0.006

*Denote significant differences between species.[1]Due to the significant differences in total length (P = 0.0002), we standardized velocity by total length and report in body lengths · s^{-1} and tail beat amplitude by total length leaving this a dimensionless variable.